At the Interface of Organic and Inorganic Chemistry: Bioinspired Synthesis of Composite Materials

Lara A. Estroff and Andrew D. Hamilton*

Department of Chemistry, Yale University, P.O. Box 208107, New Haven, Connecticut 06520-8107

Received February 1, 2001. Revised Manuscript Received April 10, 2001

The design of artificial models of the processes of biomineralization has resulted in the union of inorganic materials research and supramolecular organic chemistry. Recent work in this field of bioinspired synthesis of composite organic/inorganic materials is reviewed and prospects for the future are discussed. Attention is focused on the use of self-assembled organic superstructures to template inorganic materials with controlled morphologies.

1. Introduction

Many organisms synthesize organic/inorganic composites for the generation of protective structures. They exert exceptional control over the gross morphology, physical properties, and nanoscale organization of these materials, often creating shapes that defy the strict geometrical restrictions of the 230 classical space groups.[1,2] In recent years much interest in biomineralization has been generated due to the unique strength (up to 3000 times greater than the mineral itself), resistance to fracture, and other desirable properties of biominerals.[3,4] Additionally, the participation of biomolecules in the nucleation and growth of crystals raises interesting questions with respect to molecular recognition.[5] Most notably, the proteins involved in directing the shape of these biomaterials have often evolved to recognize and bind selectively to one or more faces of the growing crystal. Because of clear applications and the opportunity to unravel this fascinating process, research into the design of supramolecular, organic assemblies to assist the growth of inorganic crystals has increased significantly in recent years.[6]

In creating model systems of biomineralization, it will be necessary to understand the rules governing the interactions involved in crystal lattice recognition. This review focuses on recent progress in the design of synthetic agents that interact in specific ways with growing minerals. We also describe the use of these molecules in the synthesis of composite organic/inorganic materials with characteristics reminiscent of some of the intricate forms found in nature (see Figure 1).

There are two primary mechanisms by which organisms exert control over the identity and morphology of their biomineral-derived structures. First, mineralization of these inorganic materials usually occurs in cells at the protoplasmic surface boundary layer. Therefore, the macroscopic (>100 μm) arrangement (and to some extent the microscopic detail) of the minerals is controlled by the interactions of cells and vesicles with each other and with the growing mineral as dictated by surface tension.[7,8] For example, the intricate silica shells of radiolarians (Figure 1a) can be understood as the result of mineralization of close-packed arrays of vesicles attached to the membrane wall. The vesicles are arranged into a thin, polygonal foam similar to a conglomeration of soap bubbles. The second mechanism involves epitaxial (templation) control by the organic matrix over which polymorph of a specific mineral is formed and on which face that crystal is nucleated. In addition, for polycrystalline systems, the organic matrix can control the orientation of the crystals with respect to each other (Figure 1b).[5,9] In mollusks, this matrix can

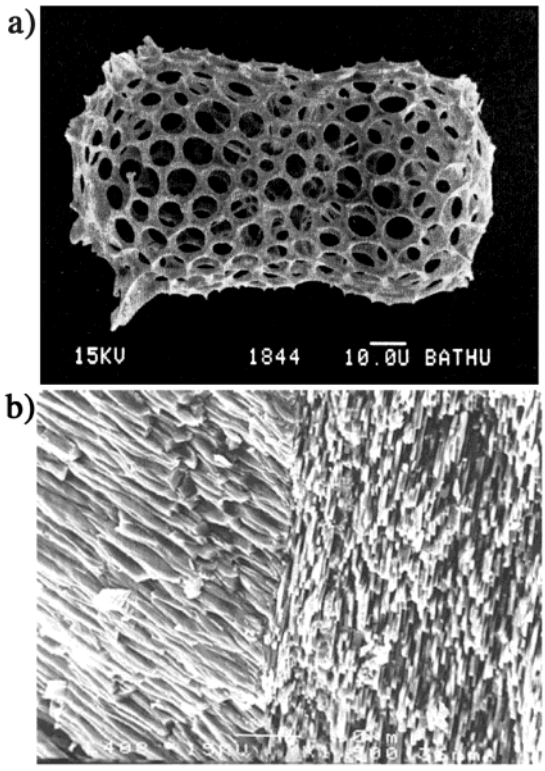

Figure 1. (a) Radiolarian microskeleton of amorphous silica, scale bar = 10 μm. (Taken from ref 4: Reproduced by permission of The Royal Society of Chemistry.) (b) Fractured surface of the shell of a bivalve mollusk, *Mytilus californianus*, showing the calcitic prismatic layer (left) and the aragonitic nacreous layers (right), scale bar = 10 μm. (Taken from ref 9: Reproduced by permission of The Royal Society of Chemistry.)

10.1021/cm010110k CCC: $20.00
Published on Web 05/23/2001

be separated into two components with different roles in the control of crystal growth. The EDTA soluble matrix is composed of primarily anionic proteins that provide the functional groups that nucleate the desired mineral and/or interact with the growing crystal faces.[10] The insoluble matrix is composed of more hydrophobic proteins and polysaccharides and provides a scaffold on which the recognition functionality is positioned in a complementary arrangement to the ionic components of the mineral. These different structural elements operate in tandem to form the complex structures within the organism.

Recent work in the field of bioinspired morphosynthesis involved both of these strategies with varying degrees of success. The most intriguing approaches have used self-assembling organic structures to template the growth of inorganic materials. In some cases the structural information from the organic assembly is directly transcribed to the inorganic material as is seen in the formation of the radiolarian skeleton (Figure 1a). In other examples, the secondary structure of the organic compound is used to precisely project functionality to interact with growing crystal faces and thus modify the morphology. The specificity, stability, and degree of organization of the organic template dictate the level of control over the morphology of the resulting inorganic materials.

2. Water-in-Oil Microemulsions, Vesicles, and Dendrimers

Water-in-oil microemulsions and vesicles formed by amphiphilic surfactants were two of the first systems used to emulate biomineralization and represent the simplest types of organic organization that have been used to template inorganic materials.[7,11−14] In a manner similar to biological systems, mineralization occurs on the surface of the vesicles and water droplets. The surface tension difference between the immiscible water and oil is controlled by the chemical structure and concentration of the surfactant. This determines the size, shape, and curvature of the vesicles and droplets, which in turn control the form of the mineralized material. Therefore, on the macroscopic scale, the materials resulting from vesicle mineralization are spherical. However, a greater diversity is found in the meso- and microscopic fine structure, depending upon the mineral being formed and the synthetic conditions.

2.1. Vesicles. The earliest approach to vesicular mineralization was reported by Ozin et al. who synthesized a lamellar aluminophosphate phase in a solution containing vesicles formed from tetraethylene glycol, amphiphilic alkylamines, and water.[7,11] The resulting material was composed of millimeter-sized spheroids with patterned surfaces (Figure 2). Both the macro- and microscopic features were attributed to participation of the vesicles in the mineralization process. The hollow microspheres act as mini-reaction vessels in which mineralization occurs due to a supersaturation of the entrapped water. Vesicles are capable of dynamic processes such as fusion and fission but their size cannot be easily controlled.[11] As a result, the potential for using this approach to synthesize specific structures is limited. However, as seen in Figure 2a, the textured surface of the resulting mineral spheroids is created by the close packing of the mineralized vesicles.

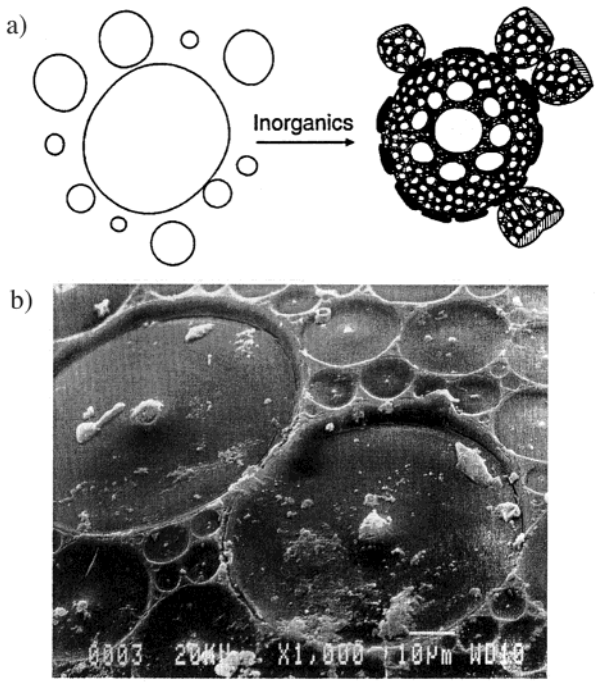

Figure 2. (a) Vesicle templating of an inorganic material. (Reprinted by permission from *Nature* (ref 8), copyright 1996, Macmillan Magazines Ltd.) (b) Magnification of the surface of a mineralized spheroid of lamellar aluminophosphate formed by a process similar to that in (a), scale bar =10 μm. (Reproduced by permission from *Nature* (ref 11), copyright 1995, Macmillan Magazines Ltd.)

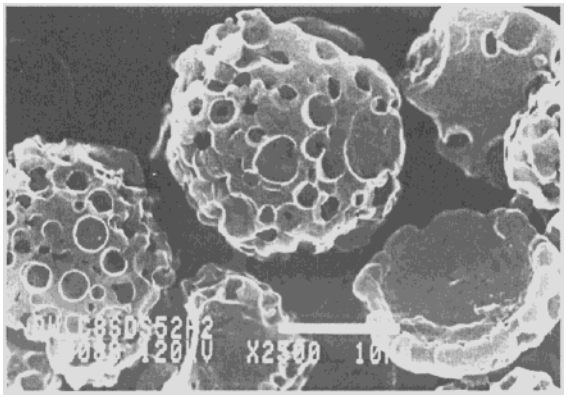

Figure 3. Vaterite spheroids formed from a microemulsion of octane:SDS:$CaHCO_3$ (71:4:25 wt %). Note the complex surface patterning and uniform size of the spheres. Scale bar = 10 μm. (Reproduced by permission from ref 14.)

2.2. Microemulsions. More recently, Mann et al. reported the morphosynthesis of calcium carbonate microsponges using a similar system.[14] Their approach involved the slow evaporation of a microemulsion, formed from a saturated aqueous solution of calcium bicarbonate in a volatile oil (octane) stabilized by sodium dodecyl sulfate (SDS). The resulting material was composed of textured spheres of vaterite, the kinetically favored, metastable polymorph of calcium carbonate (Figure 3).

The size of the vaterite spheres was found to depend on the composition of the microemulsion and thus the size of the water droplets. These take on a more uniform shape and size compared to the vesicles used by Ozin et al. This observation suggests that the precipitation

of calcium carbonate begins at the oil/water interface and moves inward rather than nucleating in the interior of the droplet. If mineral growth occurred from inside to out, the size of the spheres would show a strong dependence on the concentration of calcium bicarbonate. Furthermore, microscopic bubbles of carbon dioxide are given off upon formation of calcium carbonate from calcium bicarbonate and become trapped at the oil/water interface. The eventual escape of the gas from the vesicle creates the foamlike texture on the surface of the spheres. Vaterite is most likely formed over the other possible polymorphs because of the supersaturation inside the water droplets. This is in accordance with Ostwald's rule of stages, which predicts that the polymorph with the highest solubility will preferentially form under kinetic conditions.[15] The organic component (SDS) plays a passive role in the mineralization of the vaterite spheres, principally acting to stabilize the water droplets and, therefore, the spherical morphology.

2.3. Dendrimers. Dendrimers are a third type of spherical molecular assembly that has been used to influence the growth of calcium carbonate polymorphs.[16,17] Sommerkijk et al. modified the surface of a poly(propylene imine) dendrimer with surfactants, such as octyldecylamine, to form well-defined aggregates with a polyhedral shape and a narrow size distribution. When these persistent aggregates were injected into a supersaturated solution of calcium carbonate, amorphous calcium carbonate aggregates, which retained the original polyhedral morphology, were formed after only 15 min. This highly unstable form of calcium carbonate remained stable in solution for extended periods of time without transforming into the significantly more stable, crystalline phase calcite.[16] Even more surprising was the observation that, after 4 days, calcite rhombohedrons grown around amorphous calcium carbonate spheres were observed. The coexistence of these two phases has only been observed in biological systems and suggests a significant role for the organic component in nucleating and stabilizing the amorphous phase.

In similar work, Naka et al. used a dendrimer of poly(amidoamine) containing carboxylates on the external surface to influence the growth of calcium carbonate.[17] In their case, spherical aggregates of vaterite are formed which, similar to Sommerkijk's report, do not recrystallize to form calcite even after repeated washings with water. The linear isomer of poly(carboxylic acids) inhibits the growth of calcium carbonate, suggesting that the projection of carboxylate functionality in three dimensions by the dendrimer is crucial for the growth and stabilization of vaterite.

3. Micelles and Microarrays of Nanocrystals

Two recent reports by Mann et al. describe the synthesis of ordered microarrays of nanocrystals of both barium chromate[18] and Prussian blue [*catena*-MFe^{III}-$\{Fe^{II}(CN)_6\}$] (M = Li, Ba, K, NH_4^+)).[19] In both studies, microemulsions of water and sodium bis(2-ethylhexyl)-sulfosuccinate (AOT) are used to form reverse micelles and then to control the synthesis of the microarrays. Unlike the examples cited in the previous section, the organic component plays an active role in the organization of the nanocrystals. The crystals grow inside the water droplets and are coated by AOT molecules. As a result, they self-assemble into two- and three-dimensional, highly ordered, cubic superlattices due to interdigitation of the hydrophobic tails of AOT (see Figure 4).

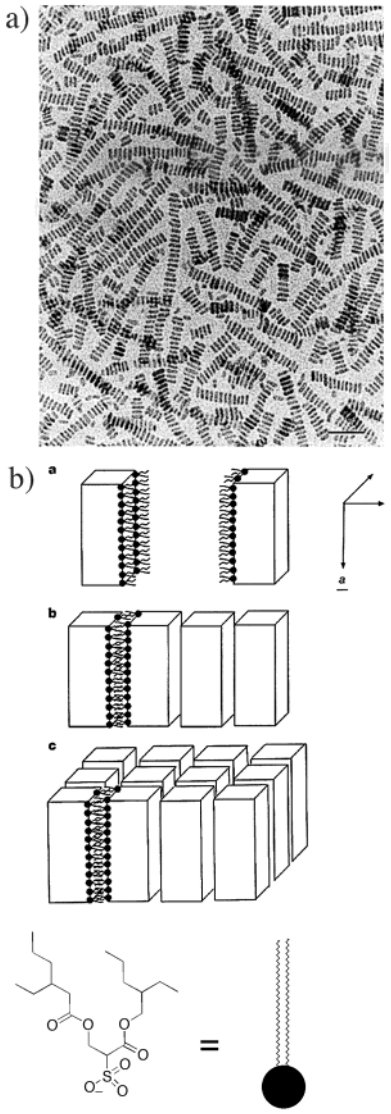

Figure 4. (a) TEM image showing ordered chains of prismatic $BaCrO_4$ prepared in AOT microemulsions. Scale bar = 50 nm. (b) Proposed model for the surfactant-induced self-assembly of nanoparticle chains and 2-D superlattices via interdigitation of the surfactant molecules coating the crystal faces. AOT molecules are shown only on one face for clarity. (Reproduced by permission from *Nature* (ref 18), copyright 1999, Macmillan Magazines Ltd.)

The size and shape of the nanocrystals are uniform and have the equilibrium morphology, prismatic and cubic, respectively, of barium chromate and Prussian blue crystals. This suggests that there is no specific interaction of the surfactant molecules with growing crystal faces. Mann et al. suggest the possibility of designing amphiphilic surfactants that are functionalized to interact specifically with the crystal faces using hydrophilic interactions and at the same time with each other using hydrophobic forces. In this way, both the morphology and the orientation of the crystals with respect to each other might be controlled.

4. Biosilicification and Artificial Systems

The second most prevalent mineral formed by organisms is amorphous hydrated silica.[20] The strategies used in biology to control the mineralization of this and other amorphous materials differ from those already discussed for the manipulation of crystalline minerals. Synthetic routes to silica involve elevated temperatures and/or extreme pH conditions. However, marine organisms are able to form silica-based structures at physiological pH and low temperatures. Recently, proteins believed to be responsible for the deposition of silica in two different families of organisms, diatoms and marine sponges, have been isolated and partially characterized.[21−24]

Diatoms are single-celled organisms with intricate cell walls composed of silica (Figure 1a). Kröger et al. have purified, after hydrogen fluoride extraction, a low molecular mass fraction of (poly)peptides that are intimately associated with the silica cell wall. Upon sequencing, it was found that the Lys residues in the peptides (named silaffins) had undergone substantial post-translational modification.[21] Polyamines with 6−11 repeats of *N*-methylpropylamine units and methylated lysines were the most common alterations. The silaffins were able to catalyze the formation of silica from silicic acid under mild conditions with the morphology of the silica being controlled by the nature of the modification within the silaffins.[22] More recently, the same group has found that different species of diatoms produce different mixtures of silaffins and accompanying polyamines. When polyamines and silaffins were mixed and matched, a variety of differently sized silica spheres were synthesized, suggesting that similar mixtures are used in vivo by the diatoms to create their intricate mineralized cell walls.

In related work, Morse and Stucky et al. have recently isolated the proteins (named silicateins) that form the insoluble, organic filaments found inside spicules from the marine sponge, *T. aurantia* (Figure 5b).[23,24] Like the silaffins, silicateins can catalyze the formation of silica at ambient conditions, but from tetraethoxysilane (TEOS) rather than silicic acid. The sequences of the silacateins are closely homologous to cathepsin L, a cysteine protease. This led the authors to look for a "catalytic triad" that could efficiently catalyze the formation of silica. The His and Asn members of the triad in cathepsin L are preserved but the Cys has been replaced with a Ser in the silicateins. Site-directed mutagenesis has confirmed that the His and Ser are essential for the catalytic activity of the silicateins, suggesting the mechanism shown in Figure 5a.[24] The silicateins therefore serve dual purposes of both providing an insoluble template for mineralization and catalyzing the formation of the amorphous silica.

4.1. Synthetic Block Copolypetides. Using the silicateins as a model, Cha et al. have designed block copolypeptides that both catalyze the formation of silica and control its morphology.[25] Initially, they found that homooligomers of L-cysteine were capable of catalyzing the formation of silica from TEOS in water at pH 7, presumably due to the nucleophilic sulfydryl group initiating the hydrolysis of TEOS in a fashion similar to the proposed mechanism shown in Figure 5a. However, silica formed via this route is an amorphous

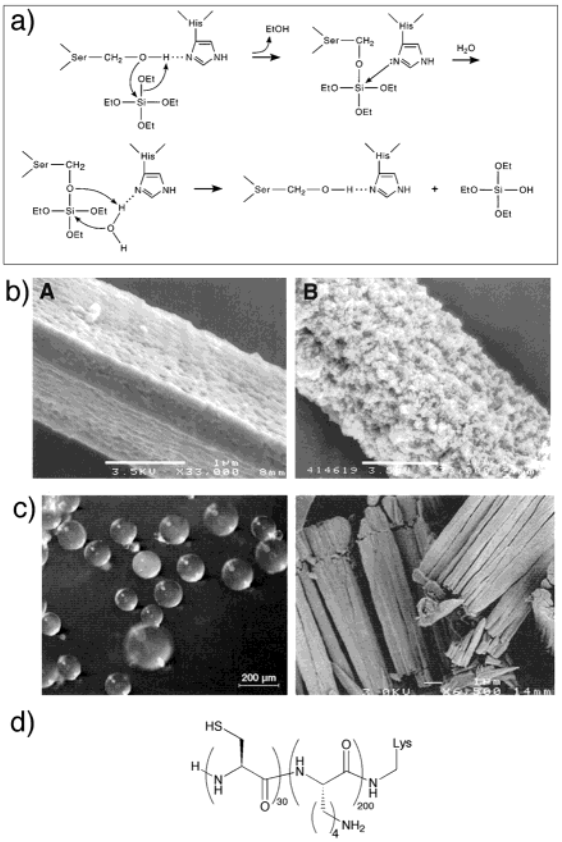

Figure 5. (a) The proposed catalytic mechanism for the hydrolysis of TEOS by the silicateins. (Reproduced by permission from ref 24.) (b) SEM image of an unmineralized organic filament isolated from inside the marine sponge spicules (left), SEM image of a mineralized filament after a 12-h reaction with TEOS (1.0 mL; 4.5 mmol) plus Tris·HCl buffer (right). Scale bars: 1 μm. (Reproduced by permission from ref 23, copyright 1999, National Academy of Sciences, U.S.A.) (c) Optical micrograph of silica spheres obtained from synthesis under nitrogen in the presence of 5 mg/mL Cys-Lys block copolymer. Scale bar: 200 μm (left). SEM image of packed silica columns from synthesis under air in the presence of the same polymer (left). Scale bar: 1 μm. (Reproduced by permission from *Nature* (ref 25), copyright 2000, Macmillan Magazines Ltd.). (d) The Cys-Lys block copolymer used in the synthesis of the silica shown in (c).

powder with no defined morphology. In the second-generation polymers, they included a hydrophilic block in addition to the less water-soluble, nucleophilic component to promote self-assembly of the polymer and thus morphological control over the silica. The cysteine−lysine amphiphilic block copolymers showed the highest activity for silica formation (Figure 5c,d). In addition, silica produced in the presence of the Cys-Lys block copolymer has a well-defined spherical morphology (Figure 5c). The resulting amphiphilic polymers self-assembled in water as shown by dynamic light scattering measurements. Interestingly, the morphology of the silica produced changed from hard, transparent, mesoporous spheres to ordered columns of silica when synthesized in air rather than under nitrogen (Figure 5c). It is believed that upon oxidative cross-linking of the Cys residues, the polymers undergo a morphological change (as supported by DLS) and thus the topology of the silica is also altered.

4.2. Sol−Gel Transcription of Organogel Fibers. Another approach to control the morphology of amor-

phous silica and crystalline minerals has been to design molecular structures that resemble the functionalized organic matrix used by some biomineralizing systems. To this end, polymeric and proteineous gels have been used as matrixes for studying the formation of inorganic minerals.[26−31] The network of pores created by a gel[32] is analogous to the postulated structure of the insoluble organic matrix in certain biomineralizing systems.[33]

Low molecular weight organic gelators have been the focus of much attention in recent years.[34−36] The property of organogelation usually arises from the self-assembly of small molecules, via hydrogen-bonding, $\pi-\pi$ stacking, or charge-transfer interactions, into fibers which, like polymer gels, become entangled, trapping solvent. The formation of these self-assembling fibers requires a stabilizing intermolecular interaction and represents a balance between the tendency of the molecules to dissolve or to precipitate in a given solvent.

Recently, there have been several published reports, primarily from Shinkai et al., of the successful mineralization of gelator fibers and other morphologies using sol−gel methods to create silica and titanium oxide fibers, tubes, and spheres.[37−44] Unlike micelles and vesicles, organogel fibers are well-defined, stable organic superstructures. The inorganic phase that forms around these structures is thus a replica of the organic assembly, including, in some cases, faithful reproduction of the helical character of chiral organic fibers (Figure 6a,b). These are the first reported examples of helical silica constructs resulting from the direct transcription of a helical, self-assembled organic structure.[37,38,40]

In common with many biominerals, the synthesis of these examples relies on electrostatic interactions between the organic template (positive charges displayed on the outside of the fibers) and the inorganic component (anionic silica). Upon calcination to remove the organic component, the helical silica structure remained. Transmission electron microscopy (TEM) images revealed them to be hollow tubes, confirming that the silica structures are transcribed directly from the helical organogel fibers (Figure 6c).

Shinkai et al.'s approach demonstrates the most active role for the organic matrix in dictating the form of the mineralized structure of those presented so far. By including positive charges on the surface of the organogel fibers, they created an integral relationship between the organic and inorganic components, reminiscent of the proposed intercalation of biological macromolecules into biominerals.[45,46] At this point, only amorphous silica and titanium oxide have been synthesized using this strategy. However, it should also be possible to use organogel matrixes to influence the growth of more ordered, crystalline materials.

The move from amorphous silica to other biological minerals (including polymorphs of calcium carbonate and calcium phosphate minerals) will require the synthesis of organic molecules that gel water.[47−50] Such organic hydrogelators should preferably display recognition domains on the fibers that will either nucleate the growth of a given mineral or interact strongly and specifically with growing crystal faces, thus altering the morphology of the crystal in a controlled fashion. The design of such a gelator should involve the incorporation of mineral binding functionality (e.g., carboxylate, phosphate, or sulfate) into an easily synthesizable, self-assembling molecule. The resulting aqueous gel would form a matrix with functionality projected into the pores. The one-component scaffold created by the aggregation of these molecules in water would be well-suited for studying mineralization in an environment where the type and density of functionality as well as the pore size could be manipulated. Our laboratory has had recent success using bis-urea dicarboxylic acid hydrogelators[47] as matrixes for the growth of calcium carbonate. The results indicate that it is possible to control which polymorph of calcium carbonate (vaterite, aragonite, or calcite) is formed inside of the gel by modulating the ratio of carboxylate ions (the gelator concentration) to calcium cations.[51]

5. Crystalline Biominerals and Conformationally Constrained Synthetic Systems

Key protein secondary structures such as α-helices and β-sheets are stabilized by a network of hydrogen bonds that influence the overall shape of the amino acid sequence. These structures are particularly attractive to chemists as a means to exert control over the presentation of binding functionality in space and to influence processes such as inorganic crystal growth. The secondary structure of the proteins in the soluble fraction of the mineralizing matrix is thought to play an important role in some biomineralizing systems. The antifreeze proteins that are expressed by organisms living in cold climates recognize and bind to ice nuclei through a variety of secondary structures.[52−55] For example, a family of these proteins (Type I) uses an α-helix to project a number of threonine and hydrophobic residues with the appropriate orientation and spacing to bind to a specific face of ice.[56−58] As a result of binding, further growth of the ice seed crystal is effectively inhibited. It has also been hypothesized that β-sheets play an important role in projecting the carboxylates of aspartic acid residues in such a way as to nucleate the growth of calcite or aragonite (another polymorph of calcium carbonate) in mollusk shells.[10,59,60]

Over the past several years, several small organic molecules,[61,62] polymers,[25,63−70] and peptides[71,72] have been prepared that are conformationally constrained in a way that emulates different protein secondary structures. In several cases, these designed compounds either nucleate the growth of specific minerals or alter the morphology of growing crystal faces by selective absorption onto a chosen face. There is also an extensive body of literature on the elegant use of monolayers (both SAMs[73] and Langmiur−Blodgett monolayers[74−78]) to template the crystallization of minerals in a controlled fashion. This work has already been reviewed[79,80] and is beyond the scope of the current review.

5.1. Small Molecules. The use of designed, small molecule additives to alter the growth of organic crystals is a well-developed field.[81,82] However, the application of such techniques to inorganic crystal growth is more difficult because of the lack of complexity of the individual components and the simple nature of the surface packing patterns.[83] In the early part of the last century, France and co-workers were interested in understanding why certain dyes were adsorbed on specific faces of

inorganic crystals during their growth.[84,85] In a series of papers, they amassed a large amount of qualitative data. The conclusions they reached regarding the role of electrostatic interactions in directing the adsorption of dyes to specific faces represent the first steps toward the design of small molecule additives to alter the growth of inorganic crystals.

It was not until the early 1990s that significant work was again done in identifying and designing small molecule inhibitors for inorganic crystals.[83,86,87] Davey et al. reported the design of a molecule that modified the growth of barium sulfate (barite).[83] First a series of carboxylates, phosphonates, and sulfonates were tested as possible inhibitors of crystal growth. Only diphosphonates were found to have specific effects on the morphology of the barite crystals. By observing which new faces were expressed, the authors were able to identify the surface to which the diphosphonates were binding. Using molecular modeling, they showed that in addition to electrostatics (the replacement of the doubly negative sulfate with a doubly negative phosphate), a good geometrical and stereochemical match of the inhibitor to the growing face is required for effective growth modification. They hypothesized that molecules with two recognition motifs, properly spaced, would be more effective than the first-generation molecules. As predicted, the ability of bis(diphosphonates) to inhibit barite growth was directly related to the linker length with only those molecules containing linkers long enough to span two binding sites, inhibiting growth. In related work, Kahr et al. analyzed a series of dye molecules known to stain dipotassium sulfate crystals on specific faces.[86,87] They identified a critical arrangement of sulfonates that superimposed nicely onto a similar arrangement of sulfates in the dipotassium sulfate lattice. From this observation they then correctly predicted several other dyes that would give similar staining patterns. The stained crystals have potential application as solid-state dye lasers.[87]

In a recent paper, Whiting et al. report the design of a small, flexible molecule, for the purpose of recognizing and binding to all of the important growing faces of barite, and thus promoting isotropic growth.[61] A family of macrocyclic aminomethylphosphonates were chosen as good candidates because previous work had shown that the phosphonate group is a good match for sulfate sites in the barium sulfate lattice.[83,88] In addition, the inherent flexibility of macrocyles would allow them to adopt a wide range of conformations to match the different lattice spacings of the faces. Using energy minimization and molecular dynamics calculations of the binding of the macrocycles to all eight faces of barium sulfate, they identified macrocycle **3** to be the best candidate for a universal face-binding agent (Figure 7).

They predicted that, in the presence of **3**, the anisotropy of the growth, which usually produces well-faceted, rhombohedral crystals of barium sulfate, would give way to isotropic growth, with all three orthogonal directions inhibited. The data supported their hypothesis and in the presence of 96 μM of **3**, spherical crystals, with no evidence of faceting, were grown exclusively.

5.2. Polymers. Ueyama et al. have designed several polyamide ligands with carboxylates that interact with

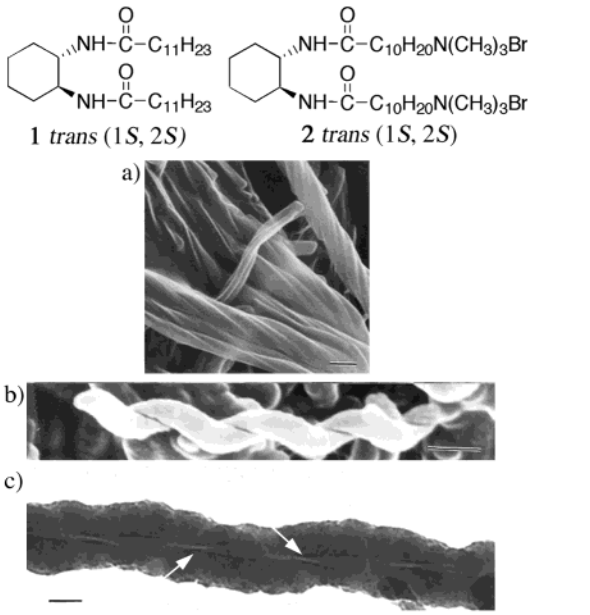

Figure 6. (a) SEM image of the helical xerogel of **1**+**2** (1:1 wt %) obtained from acetonitrile, scale bar = 200 nm. (b) SEM image of the helical silica structure obtained by sol−gel transcription of **1**+**2** (1:1 wt %) organogel fibers after calcination, scale bar = 200 nm. (c) TEM image of the silica structure obtained by sol−gel transcription of **1**+**2** (1:1 wt %) organogel fibers after calcination. Note the inner tubular structure with matching helicity, scale bar = 50 nm. (Reproduced by permission from ref 40.)

calcite crystals.[67,70] They have studied these composites using ^{13}C cross-polarization/magic angle spinning solid-state NMR. The NMR data established that polyamide **4** is incorporated into the calcium carbonate lattice, while **5** is not. In addition, only the calcite crystals grown in the presence of **4** show the expression of new faces, again suggesting that there is a favorable interaction between **4** and the growing calcite crystals.[67] On the basis of the minimized structures of the two polyamides, the authors propose that **4** is able to interact with the {001} faces of calcite because of the appropriately spaced, parallel-oriented carboxylate groups that are not present in **5** due to the trans geometry of the fumaryl spacer (Figure 8).

Double-hydrophilic block copolymers have also been successfully used to modulate the morphologies of inorganic materials including calcium carbonate,[66,68] barium sulfate,[89] and calcium phosphate.[65] The morphology of the crystals that are formed appears to depend on the ratio of [polymer]/[calcium carbonate] and the pH of the solution.[68] These variables presumably modulate the shape of the polymer aggregate in solution and thus its interactions with the growing minerals.[6]

5.3. Peptides. Laursen and DeOliveira have reported an excellent example of harnessing protein secondary structure to control the orientation of functionality so that it can bind to a targeted crystal face. Using an α-helical sequence from an antifreeze protein, they substituted aspartic acid residues for the threonines, which in the wild-type are critical for ice inhibition.[71] The expectation was that while hydroxyl groups were optimal for binding to the ice lattice, anionic carboxylates would be preferred for orienting the calcium ions on the calcium carbonate surface. The resulting helix

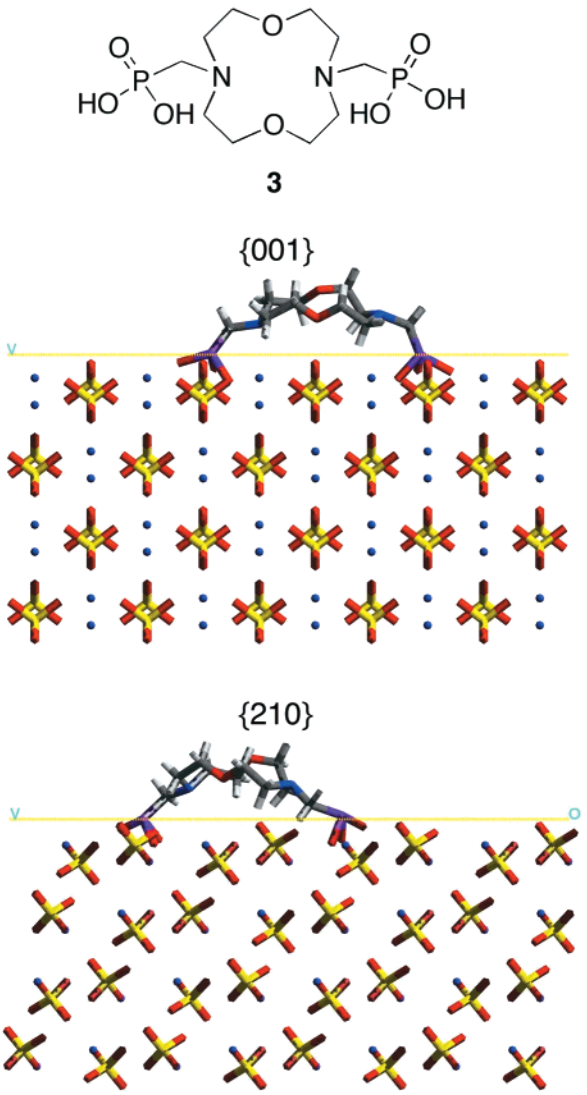

Figure 7. 1,7-Dioxo-4,10-diaza-12-crown-4-*N*,*N*′-dimethylenephosphonate **3** binding to two of the crystallographic faces of barium sulfate, as indicated. Each snapshot was captured after 10 ps of molecular dynamics performed at 300 K, following energy minimization. Color key: gray, carbon; white, hydrogen; red, oxygen; blue in modifier, nitrogen; pink, phosphorus; blue in crystal lattice, barium; yellow, sulfur. (Reproduced by permission from ref 61, copyright 2000, American Chemical Society.)

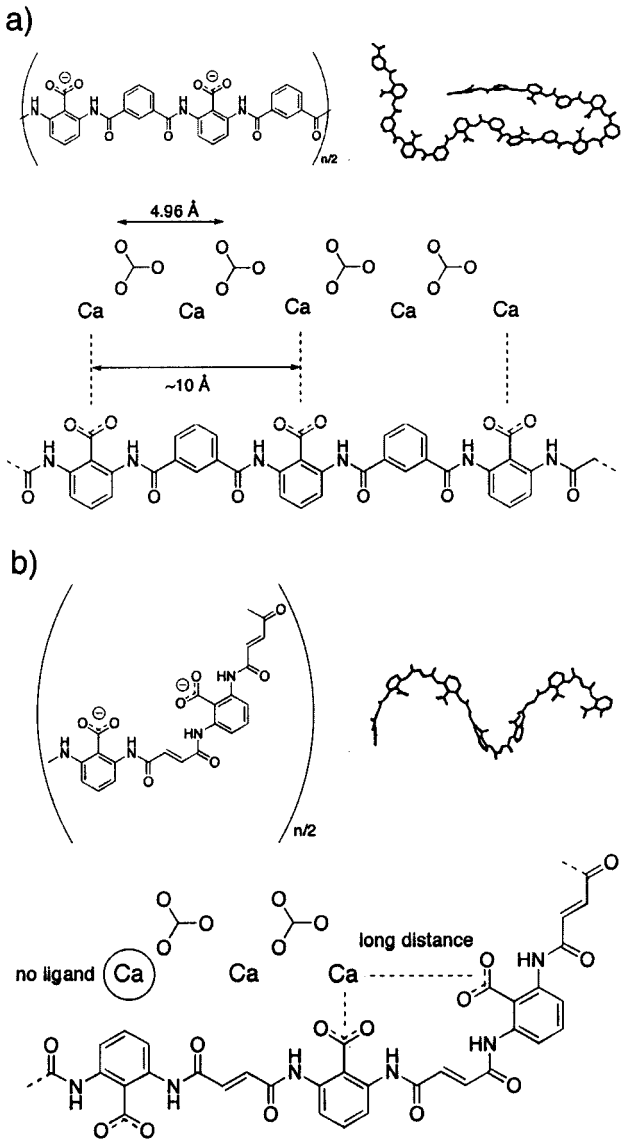

Figure 8. (a) The MD minimized structure of the polyamide $\{NHC_6H_3(COO^-)NHCO\text{-}m\text{-}C_6H_4CO\}_n$ (top) and the hypothesized, favorable interaction of this polyamide interacting with the {001} face of calcite (bottom). (b) The MD minimized structure of the polyamide $\{NHC_6H_3(COO^-)NHCOCH{=}CHCO\}_n$ (top) and the hypothesized, unfavorable interaction of this polyamide interacting with the {001} face of calcite (bottom). (Reproduced by permission from ref 67, copyright 1998, American Chemical Society.)

projects these carboxylates in a manner complementary to the carbonate layers in the $\{1\bar{1}0\}$ faces of calcite (Figure 9).

When seed crystals of calcite were grown in the presence of this designed peptide at 3 °C (where the peptide is 89% helical by circular dichroism spectroscopy), new faces, which resemble either {110} or $\{1\bar{1}0\}$ faces, appear. In fact, it is impossible to precisely identify the faces because of a lack of well-defined geometries. Most likely, multiple faces in the {*hk*0} family are expressed. The appearance of new faces results when growth in those directions is inhibited due to bound peptide, blocking the addition of more calcium or carbonate ions to the developing faces. When the experiment was repeated at 25 °C (where, by CD spectroscopy, the peptide is only 40% helical), this specific effect no longer occurs. Instead, epitaxial overgrowth on each of the original {104} faces was observed. Moreover, when other anionic, but nonhelical, peptides were used, similar epitaxial growth was observed. These results emphasize the importance of the helical secondary structure on the function of the designed peptide.

An alternative to the design approach is to screen libraries of potential crystal binding peptides. Belcher et al. have identified peptides that recognize mineral surfaces, in particular semiconductors, using a combinatorial strategy.[90] By employing phage display, they screened approximately 10^9 12-mer random peptides and identified those sequences that selectively bound specific faces of GaAs, InP, and Si crystals. For example, clones were selected that showed preferential binding to GaAs(100) ove, not only Si(100) but also GaAs(111). The authors anticipated that peptides of this length (12

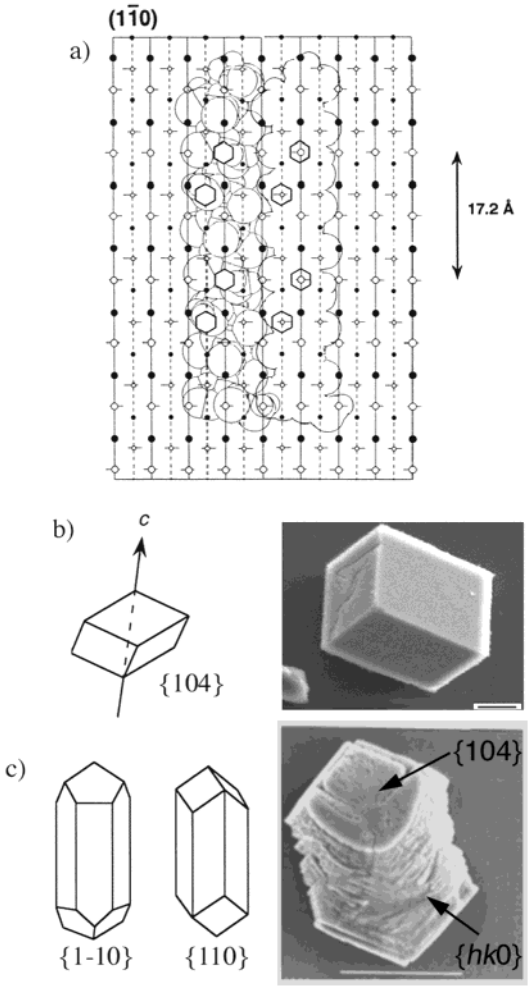

Figure 9. (a) The footprint of two of the engineered α-helices binding to one of the {1$\bar{1}$0} faces of calcite. The hexagons represent the peptide carboxylate ions that are proposed to occupy carbonate sites (indicated by unfilled circles) on the crystal face. The filled circles are calcium ions. This is a corrugated surface with the large circles in the plane of the paper and the smaller circles 1.26 Å behind the plane. (b) A schematic representation of the equilibrium calcite habit with six {104} rhombohedral faces expressed. A SEM image of such a crystal is shown as well, scale bar = 5 μm. (c) Schematic representations of elongated calcite crystals with new {1$\bar{1}$0} (left) and {110} (right) faces expressed. A SEM image of an elongated calcite crystal, with rhombohedral caps, formed from a seed crystal at 3 °C in saturated $Ca(HCO_3)_2$, in the presence of the designed calcite-binding, helical peptide (0.2 mM peptide), scale bar = 10 μm. (Reproduced by permission from ref 71, copyright 1997, American Chemical Society.)

residues) would adopt an extended conformation upon binding to the semiconductor surface. Recently, they began exploring libraries of cyclic peptides (7-mers) in which the conformation of the ring is constrained by an intramolecular disulfide bond. This approach should help to identify not only sequences but also geometries that are specific to given inorganic surfaces. Screening large combinatorial libraries (whether natural or synthetic) has the potential to elucidate the connection between sequence and secondary structure in the recognition of mineral surfaces and perhaps help us understand the relative importance of both factors. This technology may also be used to manipulate the properties of semiconductor nanoparticles and to arrange them in ordered arrays and patterns.

5.4. Future Prospects: Peptidomimetics. A serious limitation in the use of synthetic or combinatorial peptides to control crystal growth is the relative instability of secondary structure conformations in short sequences. Natural peptides shorter than 20 α-amino acids show little helical structure in water at room temperature, even when their sequences contain residues with high helical propensities.[91,92] Similarly, β-sheet structures show little stability in short peptides and few effective model systems have been formed. An important research goal in this field of bioinspired crystal engineering will be the design, synthesis, and evaluation of non-peptide scaffolds[93] that mimic the structure and function of the critical regions of biomineralizing proteins. These peptidomimetics must be conformationally constrained and project functionality in a manner similar to an α-helix or β-sheet when binding to a mineral surface. The challenge also exists to develop methods to immobilize these scaffolds since it has been shown that the same small molecule that inhibits crystal growth in solution can nucleate crystals when on solid support. In the field of enzyme inhibition and medicinal chemistry, many peptidomimetics have been developed that bind to their protein or DNA targets more strongly than the peptide sequence on which they are based.[94] Once strategies for controlling the position of binding groups in an extended and repetitive manner have been identified, we can look forward to peptide or protein mimetics that influence crystal growth and morphology more effectively than the natural biomineralizing proteins.

6. Conclusion

Chemists working at the interface of organic and inorganic chemistry have developed several techniques in recent years that enable the synthesis of inorganic materials with controlled morphologies. In this review we have presented the use of four different types of organic assemblages: vesicles, micelles, microemulsions, organogels, and conformationaly defined peptides, polymers, and small molecules. The stability and specificity of the organic superstructure directly affect the properties of the composite material. Prospects for the future include the design of more elaborate templates with the ability both to dictate the shape of the inorganic materials and to organize the particles with respect to each other. In this way not only will a greater understanding of the biological materials be reached but novel materials with useful properties will be created.

Acknowledgment. We thank the National Science Foundation (CHE9817240) for financial support of this work. L.A.E. thanks the ACS Organic Chemistry Division and Smith Kline Beecham for her graduate fellowship.

References

(1) Mann, S.; Webb, J.; Williams, R. J. P. *Biomineralization: Chemical and Biochemical Perspectives*; VCH Publishers: New York, 1989; p 541.
(2) Lowenstam, H. A.; Weiner, S. *On Biomineralization*; Oxford University Press: New York, 1989.
(3) Mann, S.; Archibald, D. D.; Didymus, J. M.; Douglas, T.; Heywood, B. R.; Meldrum, F. C.; Reeves, N. J. *Science* **1993**, *261*, 1286−1292.

(4) Mann, S. *J. Chem. Soc., Dalton Trans.* **1997**, 3953−3961.
(5) Addadi, L.; Weiner, S. *Stereochemical and Structural Relations Between Macromolecules and Crystals in Biomineralization*; Mann, S., Ed.; VCH: New York, 1989; pp 133−152.
(6) Mann, S. *Angew. Chem., Int. Ed.* **2000**, *39*, 3392−3406.
(7) Ozin, G. A. *Acc. Chem. Res.* **1997**, *30*, 17−27.
(8) Mann, S.; Ozin, G. A. *Nature* **1996**, *382*, 313−318.
(9) Weiner, S.; Addadi, L. *J. Mater. Chem.* **1997**, *7*, 689−702.
(10) Miyamoto, H.; Miyashita, T.; Okushima, M.; Nakano, S.; Morita, T.; Matsushiro, A. *Proc. Natl. Acad. Sci. U.S.A.* **1996**, *93*, 9657−9660.
(11) Oliver, S.; Kuperman, A.; Coombs, N.; Lough, A.; Ozin, G. A. *Nature* **1995**, *378*, 47−50.
(12) Walsh, D.; Hopwood, J. D.; Mann, S. *Science* **1994**, *264*, 1576−1578.
(13) Walsh, D.; Mann, S. *Nature* **1995**, *377*, 320−323.
(14) Walsh, D.; Lebeau, B.; Mann, S. *Adv. Mater.* **1999**, *11*, 324−328.
(15) Bernstein, J.; Davey, R. J.; Henck, J. O. *Angew. Chem., Int. Ed* **1999**, *38*, 3441−3461.
(16) Donners, J. J. J. M.; Heywood, B. R.; Meijer, E. W.; Nolte, R. J. M.; Roman, C.; Schenning, A. P. H. J.; Sommerdijk, N. A. J. M. *Chem. Commun.* **2000**, 1937−1938.
(17) Naka, K.; Tanaka, Y.; Chujo, Y.; Ito, Y. *Chem. Commun.* **1999**, 1931−1932.
(18) Li, M.; Schnablegger, H.; Mann, S. *Nature* **1999**, *402*, 393−395.
(19) Vaucher, S.; Li, M.; Mann, S. *Angew. Chem., Int. Ed.* **2000**, *39*, 1793−1796.
(20) Perry, C. C.; Keeling-Tucker, T. *J. Biol. Inorg. Chem.* **2000**, *5*, 537−550.
(21) Kroger, N.; Deutzmann, R.; Sumper, M. *Science* **1999**, *286*, 1129−1132.
(22) Kroger, N.; Deutzmann, R.; Bergsdorf, C.; Sumper, M. *Proc. Natl. Acad. Sci. U.S.A.* **2000**, *97*, 14133−14138.
(23) Cha, J. N.; Shimizu, K.; Zhou, Y.; Christiansen, S. C.; Chmelka, B. F.; Stucky, G. D.; Morse, D. E. *Proc. Natl. Acad. Sci. U.S.A.* **1999**, *96*, 361−365.
(24) Zhou, Y.; Shimizu, K.; Cha, J. N.; Stucky, G. D.; Morse, D. E. *Angew. Chem., Int. Ed.* **1999**, *38*, 780−782.
(25) Cha, J. N.; Stucky, G. D.; Morse, D. E.; Deming, T. J. *Nature* **2000**, *403*, 289−292.
(26) Iijima, M.; Moriwaki, Y. *J. Cryst. Growth* **1998**, *194*, 125−132.
(27) Iijima, M.; Moriwaki, Y. *J. Cryst. Growth* **1999**, *198/199*, 670−676.
(28) Wada, N.; Okazaki, M.; Tachikawa, S. *J. Cryst. Growth* **1993**, *132*, 115−121.
(29) Wada, N.; Yamashita, K.; Umegaki, T. *J. Colloid Interface Sci.* **1999**, *212*, 357−364.
(30) Fernandez-Diaz, L.; Putnis, A.; Prieto, M.; Putnis, C. V. *J. Sed. Res.* **1996**, *66*, 482−491.
(31) Kniep, R.; Busch, S. *Angew. Chem., Int. Ed. Engl.* **1996**, *35*, 2624−2626.
(32) Flory, P. J. *J. Discuss. Faraday Soc.* **1974**, *57*, 7−18.
(33) Falini, G.; Fermani, S.; Gazzano, M.; Ripamonti, A. *Chem. Eur. J.* **1997**, *3*, 1807−1814.
(34) Terech, P.; Weiss, R. G. *Chem. Rev.* **1997**, *97*, 3133−3159.
(35) van Esch, J. H.; Feringa, B. L. *Angew. Chem., Int. Ed. Engl.* **2000**, *39*, 2263−2266.
(36) Abdallah, D. J.; Weiss, R. G. *Adv. Mater.* **2000**, *12*, 1237−1247.
(37) Jung, J. H.; Ono, Y.; Hanabusa, K.; Shinkai, S. *J. Am. Chem. Soc.* **2000**, *122*, 5008−5009.
(38) Jung, J. H.; Ono, Y.; Shinkai, S. *Angew. Chem., Int. Ed. Engl.* **2000**, *39*, 1862−1865.
(39) Jung, J. H.; Ono, Y.; Sakurai, K.; Sano, M.; Shinkai, S. *J. Am. Chem. Soc.* **2000**, *122*, 8648−8653.
(40) Jung, J. H.; Ono, Y.; Shinkai, S. *Chem. Eur. J.* **2000**, *6*, 4552−4557.
(41) Kobayashi, S.; Hanabusa, K.; Hamasaki, N.; Kimura, M.; Shirai, H.; Shinkai, S. *Chem. Mater.* **2000**, *12*, 1523−1525.
(42) Clavier, G. M.; Pozzo, J. L.; Bouas-Laurent, H.; Liere, C.; Roux, C.; Sanchez, C. *J. Mater. Chem.* **2000**, *10*, 1725−1730.
(43) Jung, J. H.; Nakashima, K.; Shinkai, S. *Nano Lett.* **2001**, *1*, 145−148.
(44) Moreau, J. J. E.; Vellutini, L.; Man, M. W. C.; Bied, C. *J. Am. Chem. Soc.* **2001**, *123*, 1509−1510.
(45) Aizenberg, J.; Hanson, J.; Koetzle, T. F.; Weiner, S.; Addadi, L. *J. Am. Chem. Soc.* **1997**, *119*, 881−886.
(46) Albeck, S.; Aizenberg, J.; Addadi, L.; Weiner, S. *J. Am. Chem. Soc.* **1993**, *115*, 11691−11697.
(47) Estroff, L. A.; Hamilton, A. D. *Angew. Chem., Int. Ed.* **2000**, *39*, 3447−3450.
(48) Menger, F. M.; Caran, K. L. *J. Am. Chem. Soc.* **2000**, *122*, 11679−11691.
(49) Bhattacharya, S.; Acharya, S. N. G. *Chem. Mater.* **1999**, *11*, 3504−3511.
(50) Oda, R.; Huc, I.; Candau, S. J. *Angew. Chem., Int. Ed.* **1998**, *37*, 2689−2691.
(51) Estroff, L. A.; Hamilton, A. D., unpublished results.
(52) Yeh, Y.; Feeney, R. E. *Chem. Rev.* **1996**, *96*, 601−617.
(53) Madura, J. D.; Baran, K.; Wierzbicki, A. *J. Mol. Recognit.* **2000**, *13*, 101−113.
(54) Graether, S. P.; Kuiper, M. J.; Gagne, S. M.; Walker, V. K.; Jia, Z. C.; Sykes, B. D.; Davies, P. L. *Nature* **2000**, *406*, 325−328.
(55) Liou, Y. C.; Tocilj, A.; Davies, P. L.; Jia, Z. C. *Nature* **2000**, *406*, 322−324.
(56) Harding, M. M.; Ward, L. G.; Haymet, A. D. J. *Eur. J. Biochem.* **1999**, *264*, 653−665.
(57) Chao, H. M.; Houston, M. E.; Hodges, R. S.; Kay, C. M.; Sykes, B. D.; Loewen, M. C.; Davies, P. L.; Sonnichsen, F. D. *Biochemistry* **1997**, *36*, 14652−14660.
(58) Zhang, W.; Laursen, R. A. *J. Biol. Chem.* **1998**, *273*, 34806−34812.
(59) Falini, G.; Fermani, S.; Gazzano, M.; Ripamonti, A. *J. Chem. Soc., Dalton Trans.* **2000**, 3983−3987.
(60) Choi, C. S.; Kim, Y. W. *Biomaterials* **2000**, *21*, 213−222.
(61) Coveney, P. V.; Davey, R.; Griffin, J. L. W.; He, Y.; Hamlin, J. D.; Stackhouse, S.; Whiting, A. *J. Am. Chem. Soc* **2000**, *122*, 11557−11558.
(62) Ben, R. N.; Eniade, A. A.; Hauer, L. *Org. Lett.* **1999**, *1*, 1759−1762.
(63) Gower, L. A.; Tirrell, D. A. *J. Cryst. Growth* **1998**, *191*, 153−160.
(64) Gower, L. B.; Odom, D. J. *J. Cryst. Growth* **2000**, *210*, 719−734.
(65) Antonietti, M.; Breulmann, M.; Glotner, C. G.; Colfen, H.; Wong, K. K. W.; Walsh, D.; Mann, S. *Chem. Eur. J.* **1998**, *4*, 2493−2500.
(66) Colfen, H.; Antonietti, M. *Langmuir* **1998**, *14*, 582−589.
(67) Ueyama, N.; Hosoi, T.; Yamada, Y.; Doi, M.; Okamura, T.; Nakamura, A. *Macromolecules* **1998**, *31*, 7119−7126.
(68) Colfen, H.; Qi, L. M. *Chem. Eur. J.* **2001**, *7*, 106−116.
(69) Stupp, S. I.; Braun, P. V. *Science* **1997**, *227*, 1242−1248.
(70) Ueyama, N.; Kozuki, H.; Doi, M.; Yamada, Y.; Takahashi, K.; Onoda, A.; Okamura, T.; Yamamoto, H. *Macromolecules* **2001**, in press.
(71) DeOliveira, D. B.; Laursen, R. A. *J. Am. Chem. Soc.* **1997**, *119*, 10627−10631.
(72) Zhang, W.; Laursen, R. A. *FEBS Lett.* **1999**, *455*, 372−376.
(73) Aizenberg, J.; Black, A. J.; Whitesides, G. H. *J. Am. Chem. Soc.* **1999**, *121*, 4500−4509.
(74) Heywood, B. R.; Mann, S. *Chem. Mater.* **1994**, *6*, 311−318.
(75) Champ, S.; Dickinson, J. A.; Fallon, P. S.; Heywood, B. R.; Mascal, M. *Angew. Chem., Int. Ed.* **2000**, *39*, 2716−2719.
(76) Berman, A.; Ahn, D. J.; Lio, A.; Salmeron, M.; Reichert, A.; Charych, D. *Science* **1995**, *269*, 515−518.
(77) Bekele, H.; Fendler, J. H.; Kelly, J. W. *J. Am. Chem. Soc.* **1999**, *121*, 7266−7267.
(78) Xu, G.; Yao, N.; Aksay, I.; Groves, J. *J. Am. Chem. Soc.* **1998**, *120*, 11977−11985.
(79) Heywood, B. R. *Template-Directed Nucleation and Growth of Inorganic Materials*; Mann, S., Ed.; VCH Publishers: New York, 1996; pp 143−173.
(80) Calvert, P.; Rieke, P. *Chem. Mater.* **1996**, *8*, 1715−1727.
(81) Weissbuch, I.; Addadi, L.; Lahav, M.; Leiserowitz, L. *Science* **1991**, *253*, 637−645.
(82) Weissbuch, I.; Popovitz-Biro, R.; Leiserowitz, L.; Lahav, M. *Lock-and-Key Processes at Crystalline Interfaces: Relevance to the Spontaneous Generation of Chirality*; Behr, J.-P., Ed.; John Wiley & Sons Ltd.: New York, 1994; Vol. 1.
(83) Davey, R. J.; Black, S. N.; Bromley, L. A.; Cottier, D.; Dobbs, B.; Rout, J. E. *Nature* **1991**, *353*, 549−550.
(84) France, W. G.; Wolfe, K. M. *J. Am. Chem. Soc.* **1941**, *63*, 1505−1507.
(85) Lash, M. E.; France, W. G. *J. Phys. Chem.* **1930**, *34*, 724−736.
(86) Kelley, M. P.; Janssens, B.; Kahr, B.; Vetter, W. M. *J. Am. Chem. Soc.* **1994**, *116*, 5519−5520.
(87) Rifani, M.; Yin, Y. Y.; Elliott, D. S.; Jay, M. J.; Jang, S.; Kelley, M. P.; Bastin, L.; Kahr, B. *J. Am. Chem. Soc.* **1995**, *117*, 7572−7573.
(88) Rohl, A. L.; Gay, D. H.; Davey, R. J.; Catlow, C. R. A. *J. Am. Chem. Soc.* **1996**, *118*, 642−648.
(89) Qi, L.; Colfen, H.; Antonietti, M. *Chem. Mater.* **2000**, *12*, 2392−2403.
(90) Whaley, S. R.; English, D. S.; Hu, E. L.; Barbara, P. F.; Belcher, A. M. *Nature* **2000**, *405*, 665−668.
(91) Andrews, M. J.; Tabor, A. B. *Tetrahedron* **1999**, *55*, 11711−11743.
(92) Zimm, B. H.; Bragg, J. K. *J. Chem. Phys.* **1959**, *31*, 526−535.
(93) Orner, B. P.; Ernst, J. T.; Hamilton, A. D. *J. Am. Chem. Soc.* **2001**, in press.
(94) Babine, R. E.; Bender, S. L. *Chem. Rev.* **1997**, *97*, 1359−1472.

CM010110K